Nonlinear frequency transduction of nanomechanical Brownian motion

Olivier Maillet, Xin Zhou, Rasul Gazizulin, Ana Maldonado Cid, Martial Defoort,* Olivier Bourgeois, and Eddy Collin†
Université Grenoble Alpes, Institut Néel-CNRS, F-38042 Grenoble, France
(Received 27 June 2017; revised manuscript received 19 September 2017; published 19 October 2017)

We report on experiments addressing the nonlinear interaction between a nanomechanical mode and position fluctuations. The Duffing nonlinearity transduces the Brownian motion of the mode and of other nonlinearly coupled ones into frequency noise. This mechanism, ubiquitous to all weakly nonlinear resonators thermalized to a bath, results in a phase diffusion process altering the motion: two limit behaviors appear, analogous to motional narrowing and inhomogeneous broadening in NMR. Their crossover is found to depend nontrivially on the ratio of the frequency noise correlation time to its magnitude. Our measurements obtained over an unprecedented range covering the two limits match the theory of Y. Zhang and M. I. Dykman [Phys. Rev. B **92**, 165419 (2015)], with no free parameters. We finally discuss the fundamental bound on frequency resolution set by this mechanism, which is not marginal for bottom-up nanostructures.

DOI: 10.1103/PhysRevB.96.165434

I. INTRODUCTION

Emerging from the tremendous development of micro- and nanotechnologies, nanoelectromechanical systems (NEMSs) have opened unique capabilities to both engineers and physicists. In the first place, they serve as ultrasensitive probes for force sensing [1] with applications, e.g., to mass, charge, and even single electronic spin detection [2–4]. In the second place, these objects are extremely fruitful (weakly) nonlinear devices that are able to implement useful functions like mechanical frequency mixing [5], amplification [6], and bit storage [7]. On the fundamental level, high-quality NEMS structures can be thought of as *model systems* in which basic phenomena can be advantageously reproduced, one example being the ubiquitous bifurcation mechanism [8–10].

Ultimately, when coupled to a quantum-limited detection scheme such as a microwave cavity or a single-electron transistor, their sensitivity can be brought to the quantum limit [11,12]. This leads to a unique platform realizing the "ultimate force detector" foreseen by Caves in the 1980s [13]. Such moving structures that are macroscopic relative to the atomic scale but follow the laws of quantum mechanics are currently under development for tests of quantum foundations [14–16]. Furthermore, they are thought to be a unique new quantum electronics component enabling, e.g., coherent photon conversion from the microwave to the optical domain [17,18].

Essentially, all applications require in the first place the resonance frequency of the mechanical mode in use to be *as stable as possible*. As such, the understanding of the sources of frequency fluctuations in nanomechanical devices becomes *an essential technical topic* [1,19–23]. But in the first place, it is also *a fundamental research goal*: the measured frequency noise in actual devices is much larger than all expectations [22,24–26], demonstrating even nonlinear features for carbon-based systems [27,28]. Thus, attempts have been made to model noise sources [29,30] or to create model experiments, experimentally demonstrating the underlying mechanisms [19,31–33].

Clever driving schemes taking advantage of nonlinearities have been devised to significantly suppress frequency noise [34,35]. But what will be an "ideally frequency-noise minimizing" nanomechanical system in the first place? We know that at lowest order, the dynamics of a mechanical structure can be described by a family of *normal modes* which are nothing but independent harmonic oscillators. Pushing to the next order, these modes are weakly nonlinear (so-called *Duffing* resonators) and are dispersively coupled to one another [36–38]. Since all of the modes are unavoidably coupled to a thermal reservoir (ideally, the same one), Brownian motion of each of the modes will transduce into a frequency noise on all the others [19,22,29,33,39] and also on itself. Even in a system realized with ideal materials with no internal sources of noise, this built-in mechanism shall fix *an ultimate limit* to the mechanical resonance frequency stability at $T \neq 0$. Only in the limit of $T \to 0$, when all the modes are in their quantum ground states, do the dispersive couplings lead to a simple frequency renormalization of the resonances through the zero-point fluctuations of each of them: a sort of *mechanical Lamb shift* that dresses all the modes [40].

In the present paper, we report on a *model experiment* in which we use very high quality silicon nitride NEMSs cooled down to Kelvin temperatures. A *single* mode is driven by a stochastic force, leading to effective temperatures as high as 10^9 K for only this mode. We extract the effect of this "artificial out-of-equilibrium heating" on the *mode itself*, both by measuring the spectrum of the motion and by measuring the simultaneous response of the same mode to a sine-wave excitation. The effect on a *nearby mode* is measured with the sine-wave excitation scheme. The setup is carefully calibrated [41], while the devices' characteristics are obtained by both measurements and calculations; the agreement with theory is obtained *with no free parameters*. In addition, the experiment is performed on different devices, proving the reproducibility of the results.

We demonstrate experimentally the two regimes of the Brownian motion transduction, named after analog phenomena present in nuclear magnetic resonance (NMR): "motional narrowing" and "inhomogeneous broadening" [31]. Based on Ref. [39] and simple expansions of the Euler-Bernoulli theory (including nonlinear coefficients [37,38,42]), we give

*Present address: CEA, LETI, MINATEC Campus, 17 rue des Martyrs, 38054 Grenoble Cedex 9, France.
†Corresponding author: eddy.collin@neel.cnrs.fr

the analytic tools enabling the calculation of the "ultimate frequency stability" reached by any doubly clamped device, depending on stress, dimensions, and temperature T [43]. For bottom-up structures like, e.g., carbon nanotubes with a high aspect ratio, this limit *is not marginal* [29].

II. RESULTS

A. The nanoelectromechanical systems

The devices under study are doubly clamped silicon nitride nanobeams with width $w = 300$ nm and thickness $e_{SiN} = 100$ nm. Two high-stress (1 GPa) beams of $L = 300$ μm length have been measured along with a 250-μm one (samples 300 μm-1, 300 μm-2 and 250 μm-1), together with one low-stress (100 MPa) $L = 15$ μm shorter beam (15 μm-1). A thin layer of aluminum (e_M about 30 to 90 nm thick) has been added on top to create electrical contacts. The experiments are performed at 4.2 K in cryogenic vacuum (pressure $<10^{-6}$ mbar).

Figure 1(a) shows a schematic of the setup. For each device and each mode n (or m) studied, we perform a careful calibration based on the technique developed in Ref. [41]. We can thus infer forces F_n and displacements x_n in SI units and compute the device characteristics (namely, mass m_n, spring constant k_n, and nonlinear coefficients $\beta_{n,m}$). These match the expected calculated values; note that particular care has been taken in the calibration of the noise source. The only fit parameter is, indeed, an overall correction of the force noise not exceeding 15% in amplitude (same order as in Ref. [10]). Actuation and detection are performed with the magnetomotive scheme [41,44]. A drive current (composed of both the Gaussian noise component centered around resonance frequency ω_1 and a sine-wave of frequency ω close to ω_n, with $n = 1$ or $n = 3$) is injected in the NEMS metallic layer through a home-made adder and a 1-kΩ bias resistor. In an in-plane dc magnetic field orthogonal to the beams, this generates an out-of-plane driving force $F_n(t)$ with harmonic component $F_n^0 \cos(\omega t)$. The motion is detected through the induced voltage by means of a standard lock-in detection. We obtain the two quadratures, in phase (X) and out of phase (Y) with respect to the local oscillator.

In order to preserve our calibration capabilities, the lock-in has also been used for the spectral measurements $S_X^n(\omega)$ of the Brownian motion of mode $n = 1$. Moreover, this enables us to measure fluctuations on each of the two quadratures, X,Y, independently (plus their cross correlations). When the sinusoidal excitation is weak (or nonexistent), the spectra on X and Y are equivalent, and no correlations are detected; this is the range of validity of the work presented here. However, signatures of squeezed statistics of motion [45] can be observed on measured spectra when the sinusoidal excitation is too large. Details on the measurement technique, calibrations, and calculated parameters can be found in the Supplemental Material [43].

B. Dispersive coupling driven by stochastic motion

Linear motion of thin nanobeams is very well described by the Euler-Bernoulli equation [46]. The basic ingredients involved are the inertia (through the density ρ_{beam}), the Young's modulus E_{beam}, and the tension T_0 generated by the in-built stress. For doubly clamped beams, the nonlinear behavior is well understood: it arises from the stretching of the device under transverse motion x [37,38,42]. This *geometric nonlinearity* results in a tensioning $T_0 + \delta T$ of the beam with $\delta T \propto x^2$, which can be incorporated into the beam equation [42]. This leads to a frequency shift of the modes that is proportional to the square of the displacement. When only two modes n,m are under study, we write

$$\omega_n = \omega_n^0 + \beta_{n,n} x_n^2 + \beta_{n,m} x_m^2, \tag{1}$$

$$\omega_m = \omega_m^0 + \beta_{m,m} x_m^2 + \beta_{m,n} x_n^2, \tag{2}$$

where we introduced the linear resonance frequencies ω_n^0,ω_m^0 and the Duffing nonlinear coefficients $\beta_{i,j}$ [38]. We remind the interested reader of the mathematical derivation of these expressions in the Supplemental Material [43].

Equations (1) and (2) can be adapted when one of the motions, say, x_n, is a stochastic variable: $x_n = x_n^0 + \delta x_n$, with x_n^0 being the certain component and δx_n being the Gaussian and centered random component. In order to introduce the phenomenon, let us first consider the case depicted in Fig. 1(b), where only one mode n is addressed. We apply on $n = 1$ a Gaussian random force $\delta F_n(t)$ of spectrum $S_F^n(\omega)$ whose strength can be converted into an effective temperature T_{eff} through the fluctuation-dissipation theorem $S_F^n = 2k_B T_{\text{eff}} m_n \Delta\omega_n$. $\Delta\omega_n$ is the linewidth of the resonance of mode n (with $Q_n = \omega_n^0/\Delta\omega_n$ being the quality factor), and $S_F^n(\omega)$ is white around only the mode studied (and negligible elsewhere). The mechanical mode thus experiences position fluctuations (Brownian motion) linked to S_F^n through the mechanical susceptibility, whose spectrum $S_X^n(\omega)$ peaks around ω_n^0. Since $T_{\text{eff}} \gg 4.2$ K, the experimental temperature, we safely neglect all other sources of fluctuations while enabling a thorough tuning of the Brownian motion amplitude of only mode n.

C. Transduction mechanism

From the Duffing equations, the random motion δx_n is transduced into a frequency noise $S_{\delta\omega}(\omega)$. Since this dependence is quadratic, the frequency noise is neither Gaussian nor centered. Its spectrum depicted in Fig. 1(b) consists of a low-frequency part and a high-frequency component that peaks around $2\omega_n$. The high-frequency fluctuations are essentially filtered out by the mode dynamics, as can be seen in a rotating-wave approximation. Thus, driving the mode with a sine-wave force $F_n^0 \cos(\omega t)$ weak enough to remain in the linear response limit, the motion x_n^0 will adiabatically follow the slow frequency fluctuations, experiencing both a frequency shift and a spectral broadening [39]. The measurement scheme itself is always slow enough to ensure that all fluctuations are spanned while acquiring data. Note that the Brownian fluctuations do not need to be small for the theory to apply.

The phenomenon is nontrivial and depends strongly on the correlation time of the fluctuations $\tau_c = 1/\Delta\omega_n$. Defining $\Sigma_{\delta\omega} = 4\beta_{n,n}\Delta x_n^2$ as a frequency noise amplitude parameter (essentially, the standard deviation $\propto [\int S_{\delta\omega} d\omega]^{1/2}$ of the stochastic frequency), two regimes should be distinguished depending on the magnitude of the product $\tau_c \times \Sigma_{\delta\omega}$ [see Fig. 1(c)]. The process can be understood in terms of phase

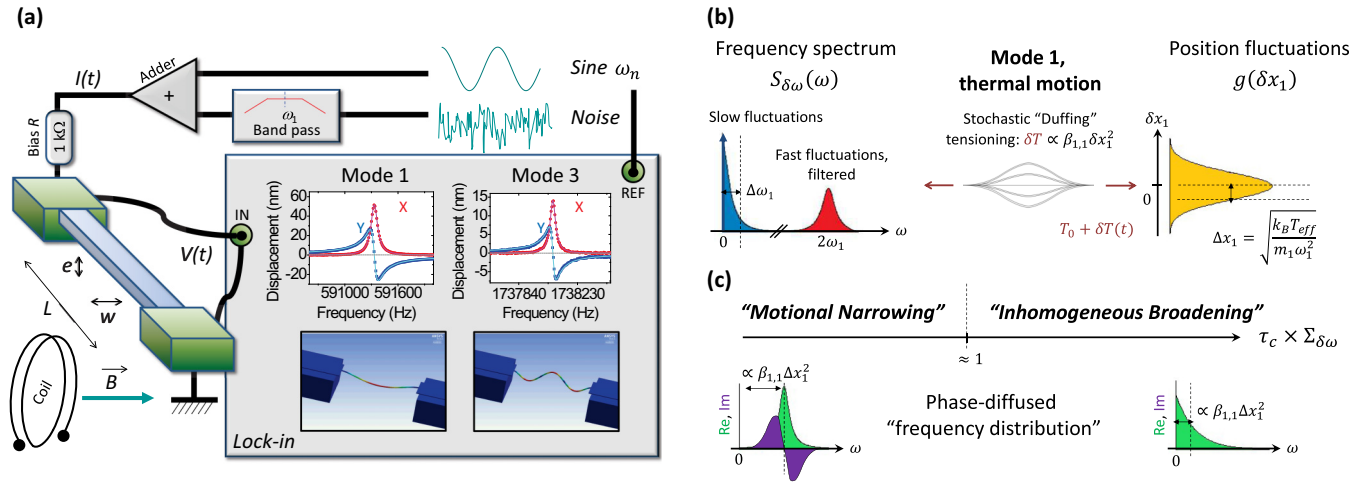

FIG. 1. (a) The nanomechanical beams (left) are driven by means of a dc magnetic field B and an ac current consisting of the sum of two components (top): a sine wave whose frequency is swept around a chosen mode ($n = 1$ or $n = 3$ here) and a Gaussian white noise filtered around mode $n = 1$. The motion is detected with a lock-in amplifier through the induced voltage V, leading to the two quadratures, X and Y, for each mode $n = 1$ and $n = 3$ (right; lines are Lorentz fits, and images are ANSYS numerical simulations). Data correspond to beam 300 μm-1 in the linear regime. (b) The Gaussian noise force applied onto the mode (here mode 1, middle) is equivalent to an effective temperature $T_{\rm eff}$ (right). The motion transduces into a frequency noise (spectrum on the left) because of the Duffing nonlinearity $\beta_{1,1}$ due to tensioning. Only the low-frequency part of these fluctuations is relevant (in blue, with the dc average marked by an arrow); the high-frequency term (red) is filtered out by the dynamics of the mode (adiabatic picture in the rotating frame of the motion). (c) Depending on the amplitude of frequency fluctuations $\Sigma_{\delta\omega}$ (their standard deviation $\propto [\int S_{\delta\omega} d\omega]^{1/2}$) with respect to their correlation time τ_c (here $1/\Delta\omega_1$, with $\Delta\omega_1$ being the linewidth of the noisy mode), two regimes are distinguished: "motional narrowing" and "inhomogeneous broadening." This is due to the underlying dynamics of phase diffusion experienced by the mechanical mode, leading to the averaged frequency distribution depicted below the horizontal arrow (green and violet).

diffusion for the mode studied, the dynamics being averaged over all realizations of the fluctuating resonance frequency $\delta\omega$, namely, $x_n^0(t) \propto \langle e^{i\int_0^t \delta\omega(t'')dt''}\rangle$ [39]. The frequency-domain data can thus be described by a convolution of the linear response by a complex-valued distribution of frequencies, as seen from the NEMS [bottom of Fig. 1(c)]:

$$\mathrm{FT}\left[\frac{\exp(+\Gamma_n t)}{\cosh(a_n t) + \frac{\Gamma_n}{a_n}(1+2i\alpha_n)\sinh(a_n t)}\right](\omega), \qquad (3)$$

where FT indicates Fourier transform, with $\Gamma_n = \Delta\omega_n/2$ being the mode's relaxation rate, $a_n = \Gamma_n\sqrt{1+4i\alpha_n}$, and $\alpha_n = \frac{\Sigma_{\delta\omega}}{2\Gamma_n} = \tau_c \times \Sigma_{\delta\omega}$ being the *motional narrowing parameter*.

By analogy with nuclear magnetic resonance, when $\tau_c \times \Sigma_{\delta\omega} \ll 1$, the certain component's dynamics is said to be in the motional narrowing (MN) limit, while for $\tau_c \times \Sigma_{\delta\omega} \gg 1$ it lies in the inhomogeneous broadening (IB) limit. In the former case, the fluctuations are too fast to enable the resolution of the small frequency changes $\Sigma_{\delta\omega}$ [31,47]: the random variable's dynamics loses memory too quickly, and only a fraction of the frequency fluctuations impacts the driven motion. This leads to a *certain* frequency shift which is nothing but the average of the frequency fluctuations proportional to Δx_n^2, together with a (weaker, second-order) symmetric broadening *quadratic* in Δx_n^2 [bottom left distribution in Fig. 1(c)]. In the latter case, the fluctuations are slow enough that the full range of frequency fluctuations can be explored by the x_n^0 sine-wave response [32,48]: there is a large asymmetric broadening, which reflects the actual distribution of frequency fluctuations [bottom right in Fig. 1(c)]. When mode $m = 3$ is sine wave driven and detected while force noise is still applied onto mode $n = 1$, the treatment is identical to the replacement $\Sigma_{\delta\omega} = 2\beta_{m,n}\Delta x_n^2$ [39]. In addition, an equation similar to Eq. (3) holds for the direct calculation of nonlinear Brownian spectra [39]. A brief description of the theoretical tools developed in Ref. [39] is given in the Supplemental Material [43].

In the next section, we present the experimental data and the theoretical calculations corresponding to these two situations. The displacement noise spectrum of mode $n = 1$ is also directly measured. We reach the limit where this spectrum itself is *imprinted by the Duffing nonlinearity* [19] and match it to the theory [39]. Since Brownian motions of two $m \neq n$ distinct modes are not correlated, from these elementary measurements one can then deduce the *generic* situation where N thermalized modes of the same structure are coupled together.

D. Measured resonance properties

In Fig. 2(a) we present the direct measurement of the Brownian noise spectra $S_X^n(\omega)$ on mode $n = 1$ for sample 300 μm-2. No sine-wave excitation is applied on either $n = 1$ or $m = 3$ modes. The noise level is quoted in terms of standard deviation Δx_1^2 instead of $T_{\rm eff}$ (or force noise intensity) since this is the physical parameter of importance. For small Brownian excitations, the peak remains Lorentzian. However, when the amplitude of motion becomes large, the nonlinear term $\beta_{1,1}$ starts to impact the line shape: the peak

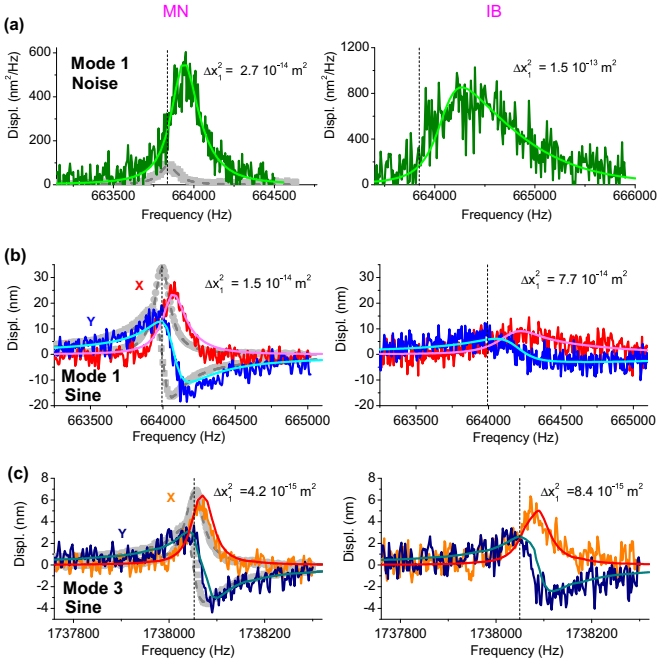

FIG. 2. (a) Brownian motion spectra measured on mode $n = 1$ of sample 300 μm-2 (Duffing spectra). (b) In-phase (X) and quadrature (Y) components measured for mode $n = 1$ while driving noise on the same $n = 1$ mode for sample 300 μm-2 (intramode). (c) Same measurement performed on mode $n = 3$ while driving fluctuations on $n = 1$ for sample 300 μm-1 (intermode coupling). The standard deviation Δx_1^2 (i.e., Brownian motion level) is increased from left to right (essentially, from the MN to IB regime; see Fig. 3), and sinusoidal drives are kept in the linear regime. The gray data are the references obtained for very weak noise levels. The vertical dashed lines are the resonance position without Brownian transduction, and other lines are theoretical calculations (see text).

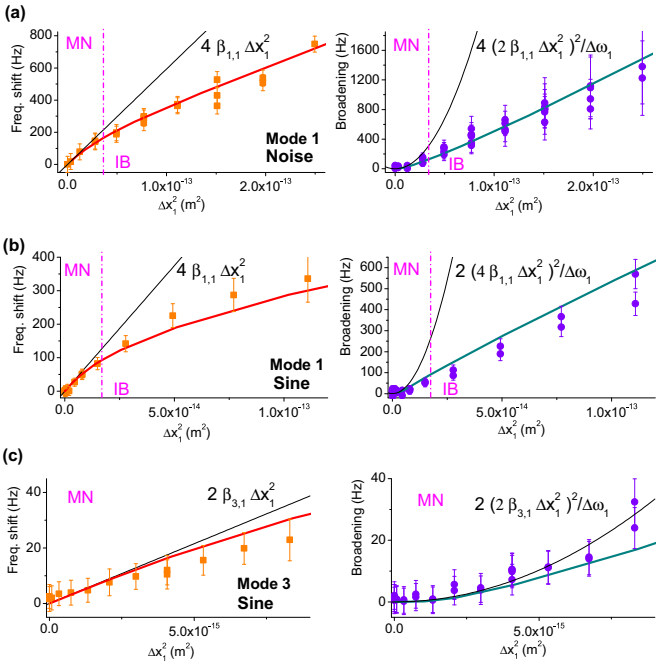

FIG. 3. Frequency shift (left) and broadening (from FWHH, right) for (a) the (Duffing) spectra measured on mode $n = 1$ for sample 300 μm-2, (b) the sine-wave excitation of mode $n = 1$, with Brownian motion on the same mode for sample 300 μm-2 (intramode case), and (c) similar result for sine-wave excitation of mode $m = 3$, with Brownian motion of mode $n = 1$ for sample 300 μm-1 (intermode). The thin lines are the motional narrowing (MN) analytic expansions, with the dot-dashed vertical lines corresponding to the crossover towards inhomogeneous broadening (IB) when $\tau_c \times \Sigma_{\delta\omega} = 1$. The solid lines are from the complete theoretical model (see text).

broadens and becomes asymmetric [19,33]. As expected, the resonance peak globally shifts towards higher frequencies [see Fig. 3(a) for a summary of the spectrum characteristics]. The lines are the exact theory from Ref. [39], computed with no free parameters: we call them *Duffing spectra* [43]. Note that no deviations from standard Gaussian statistics are measured in these conditions, which is as it should be for high-Q devices [49]: spectra on the X quadratures are equivalent to the ones measured on Y, and no cross-correlations are detected [43].

We turn next to the case of the intramode coupling. We still drive mode $n = 1$ with white noise, but we also measure and drive it with a sine-wave signal. Mode $m = 3$ is left unexcited. Data and theory from Ref. [39] are compared in Fig. 2(b) with no free parameters. The X line shapes look like the peaks obtained in the Duffing spectrum case (Fig. 2). The effect of the added force noise on the mode is again twofold: first, the resonance peak slightly shifts towards higher frequencies, and second, it broadens (consequently flattens) and acquires an asymmetric shape. In Fig. 3(b) we summarize the characteristics of the measured resonance lines on device 300 μm-2 (obtained from the X quadrature).

Measured resonance lines and calculations in the intermode case (sine-wave driving and measuring mode $m = 3$ while adding force noise on mode $n = 1$) are shown in Fig. 2(c). They resemble the intramode results of Fig. 2 very much, even though the quality of the data did not enable us to reach as high fluctuation levels [see Fig. 3(c)]. More data can be found in the Supplemental Material [43].

The three basic situations are compared in Fig. 3: we show the characteristics of the measured spectra and resonance lines on 300-μm devices in terms of frequency shift (position of the maximum of the resonance peak) and broadening (measured from the full width at half height, FWHH). The same characteristics for 250 and 15 μm devices are also shown in the Supplemental Material [43]: since the nonlinear coefficients depend strongly on the length L of the structures, the agreement between theory and experiment demonstrates the robustness of the effect.

The global agreement between data and theory is remarkable. Essentially, Duffing spectra and intramode and intermode Brownian frequency transduction display the same characteristic features. This agreement highlights that the main ingredient is the *dynamics of the noisy mode*, not the one of the chosen probe. From Fig. 3, we see that we span the whole range of the phenomenon from motional narrowing to inhomogeneous broadening. In the motional narrowing limit, indeed, the first-order effect is a global

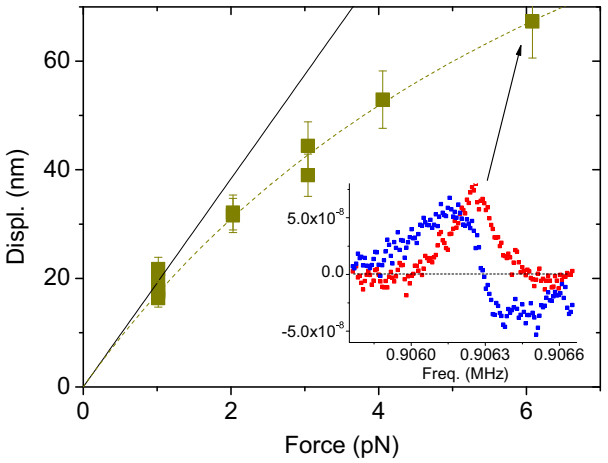

FIG. 4. Large sine-wave excitation forces. Amplitude of the sine-wave response peak as a function of excitation force for mode $n = 1$ of device 250 μm-1. Force noise is applied on the same mode, $n = 1$, such that $\Delta x_1^2 = 2.2 \times 10^{-15}$ m^2. The solid line is the linear theory, which clearly does not fit the data (squares and dashed guiding line). The inset corresponds to the largest drive measured peak.

frequency shift proportional to Δx_n^2. On the other hand, in the inhomogeneous broadening range the main feature is the asymmetric broadening, which is nothing but the image of the frequency distribution (inhomogeneity in the time domain, as opposed to the position domain for NMR [32]). Further technical discussions of these two limits can be found in the Supplemental Material [43].

However, the theory of Ref. [39] applies for sinusoidal excitation strengths lying within the linear response range. When the motion amplitude is increased beyond this limit, new phenomena are expected to take place, e.g., the parametric squeezing of the Brownian motion [45]. One signature obtained experimentally that fails to be reproduced by the theory is shown in Fig. 4: for large sine-wave excitations, the amplitude of the detected mechanical peak *lies below* the calculation, as if the impact of frequency noise were stronger than expected. In the Supplemental Material [43], we show that the noise spectra measured on mode n are indeed altered by the back-action of the sine-wave response x_n^0; the X and Y quadratures are not equivalent anymore, and cross correlations are nonzero at some peculiar frequencies. Further work, both theoretical and experimental, is required to explore this new dynamical range.

E. Application to a thermalized family of modes

For a physical thermal bath, the device is always in the motional narrowing limit. In this case, the linear response of mode n to a weak sinusoidal drive remains Lorentzian, with a resonance frequency "dressed" by the Brownian motion of all modes (global frequency shift proportional to T). This is essentially analogous to a mechanical Lamb shift [40] in the classical domain. Furthermore, the linewidth of the resonance is impacted by a T^2 term, a "thermal decoherence" effect.

Reproducing results from Ref. [39], frequency dressing and thermal decoherence can be written at lowest order in terms of simple expansions for mode n:

$$\omega_n = \omega_n^0 + 4\beta_{n,n}\Delta x_n^2 + \sum_{m\neq n} 2\beta_{n,m}\Delta x_m^2 + \sum_{m'} 2\bar{\beta}_{n,m'}\Delta y_{m'}^2, \tag{4}$$

$$\Delta\omega_n = \Delta\omega_n^0 + 2\frac{\left(4\beta_{n,n}\Delta x_n^2\right)^2}{\Delta\omega_n^0} + \sum_{m\neq n} 2\frac{\left(2\beta_{n,m}\Delta x_m^2\right)^2}{\Delta\omega_m^0} + \sum_{m'} 2\frac{\left(2\bar{\beta}_{n,m'}\Delta y_{m'}^2\right)^2}{\Delta\bar{\omega}_{m'}^0}. \tag{5}$$

The validity of these expansions has been experimentally verified in the present work for only two modes (Fig. 3). They can be extended in this simple way to many modes since the Brownian motion for $n \neq m$ is uncorrelated. For the sake of completeness, we also added the sum over the *other family of transverse modes* (in the $\vec{y}$ direction), whose coefficients are designated with an overbar and whose index is indicated with a prime (the position standard deviation is simply written $\Delta y_{m'}^2$). Indeed, the nonlinear coupling between flexural modes of different families has been studied recently [50]. We shall not discuss the coupling to longitudinal and torsional modes, which is outside of the scope of beam mechanics; these depend directly on Poisson's ratio and will be very weak.

Equations (4) and (5) can be easily evaluated for doubly clamped beams by means of mode parameters calculated using the nonlinear extension of Euler-Bernoulli beam theory [37,38,42]. With the simple equipartition result $\Delta x_n^2 = k_B T/k_n, \Delta y_{m'}^2 = k_B T/\bar{k}_{m'}$ we can rewrite these expressions such that

$$\frac{\omega_n - \omega_n^0}{\omega_n^0} \propto \left(\frac{E_{\text{beam}} A}{2L^3}\right)\frac{(k_B T)}{\left(2k_n^2\right)}, \tag{6}$$

$$\frac{\Delta\omega_n - \Delta\omega_n^0}{\Delta\omega_n^0} \propto \left(\frac{E_{\text{beam}} A}{2L^3}\right)^2\frac{(k_B T)^2}{\left(2k_n^4\right)}Q_n^2, \tag{7}$$

with $A = we$ being the cross section. In the Supplemental Material we summarize the mode parameters obtained in the two extreme limits of Euler-Bernoulli theory: low stress (beam) and high stress (string) [43]. Two key facts have to be highlighted: first, the prefactor in Eqs. (6) and (7) that gives the strength of the effect depends on material properties and strongly on *geometry*. Second, increasing the stress in the structure *does reduce* the sensitivity to Brownian transduction.

III. CONCLUSION

By artificially heating a single mode of a NEMS structure, we have demonstrated experimentally the nonlinear frequency transduction of the Brownian motion of this mode onto itself and onto a nearby one. Beyond harmonic mode coupling [36–38], the correlation time τ_c of fluctuations impacts the dynamics. Two regimes are observed depending on the strength of the stochastic force applied: motional narrowing when the frequency fluctuations are small with respect to $1/\tau_c$ and inhomogeneous broadening when they are large.

The data have been compared to the theory from Ref. [39] that spans the whole range, and we have demonstrated excellent agreement without free parameters. The present work has presented a complete experimental analysis of this fundamental (classical) phenomenon, analogous to nuclear magnetic resonance (quantum); effective temperatures up to 10^9 K for the mechanical mode under study were required to reach the inhomogeneous broadening limit.

When extending these results to the case of a family of modes thermalized to a bath at temperature T, we found that for typical high-stress top-down structures like the ones used here, the Brownian transduction phenomenon is clearly negligible. However, for much smaller low-stress structures with a high aspect ratio, the effect is foreseen to be limiting in sensing applications [43]. In addition, the certain frequency shift arising from the thermal dressing can also be a source of frequency instability if temperature T is fluctuating. Finally, when addressing the issue of *intrinsic* sources of decoherence, it is mandatory to control this phenomenon. Note that other authors reached the same conclusions with a different approach specific to nanotubes [29].

ACKNOWLEDGMENTS

We thank J. Minet and C. Guttin for help in setting up the experiment, as well as J.-F. Motte, S. Dufresnes, and T. Crozes from the facility Nanofab for help in the device fabrication. We also warmly thank M. Dykman for very useful discussions. We acknowledge support from ANR Grant MajoranaPRO No. ANR-13-BS04-0009-01 and ERC CoG Grant ULT-NEMS No. 647917. This work has been performed in the framework of the European Microkelvin Platform (EMP) collaboration.

[1] J. Moser, J. Guttinger, A. Eichler, M. J. Esplandiu, D. E. Liu, M. I. Dykman, and A. Bachtold, Nat. Nanotechnol. **8**, 493 (2013).
[2] J. Chaste, A. Eichler, J. Moser, G. Ceballos, R. Rurali and A. Bachtold, Nat. Nanotechnol. **7**, 301 (2012).
[3] A. Cleland and M. Roukes, Nature (London) **392**, 160 (1998).
[4] D. Rugar, R. Budakian, H. J. Mamin and B. W. Chui, Nature (London) **430**, 329 (2004).
[5] E. H. Krommer, A. Kraus, R. H. Blick, G. Corso, and K. Richter, Appl. Phys. Lett. **77**, 3102 (2000).
[6] R. Almbog, S. Zaitsev, O. Shtempluck, and E. Buks, Appl. Phys. Lett. **88**, 213509 (2006).
[7] I. Mahboob and H. Yamaguchi, Nat. Nanotechnol. **3**, 275 (2008).
[8] J. S. Aldridge and A. N. Cleland, Phys. Rev. Lett. **94**, 156403 (2005).
[9] C. Stambaugh and H. B. Chan, Phys. Rev. B **73**, 172302 (2006).
[10] M. Defoort, V. Puller, O. Bourgeois, F. Pistolesi, and E. Collin, Phys. Rev. E **92**, 050903(R) (2015).
[11] J. D. Teufel, T. Donner, D. Li, J. W. Harlow, M. S. Allman, K. Cicak, A. J. Sirois, J. D. Whittaker, K. W. Lehnert, and R. W. Simmonds, Nature (London) **475**, 359 (2011).
[12] M. D. LaHaye, O. Buu, B. Camarota, and K. C. Schwab, Science **304**, 74 (2004).
[13] C. M. Caves, K. S. Thorne, R. W. P. Drever, V. D. Sandberg, and M. Zimmermann, Rev. Mod. Phys. **52**, 341 (1980).
[14] A. D. O'Connell, M. Hofheinz, M. Ansmann, R. C. Bialczak, M. Lenander, E. Lucero, M. Neeley, D. Sank, H. Wang, M. Weides, J. Wenner, J. M. Martinis, and A. N. Cleland, Nature (London) **464**, 697 (2010).
[15] D. Kleckner, I. Pikovski, E. Jeffrey, L. Ament, E. Eliel, J. van den Brink, and D. Bouwmeester, New J. Phys. **10**, 095020 (2008).
[16] A. D. Armour and M. P. Blencowe, New J. Phys. **10**, 095004 (2008).
[17] J. Bochmann, A. Vainsencher, D. D. Awschalomand, and A. N. Cleland, Nat. Phys. **9**, 712 (2013).
[18] A. Rueda, F. Sedlmeir, M. C. Collodo, U. Vogl, B. Stiller, G. Schunk, D. V. Strekalov, C. Marquardt, J. M. Fink, O. Painter, G. Leuchs, and H. G. L. Schwefel, Optica **3**, 597 (2016).
[19] J. Gieseler, L. Novotny, and R. Quidant, Nat. Phys. **9**, 806 (2013).
[20] J. Moser, A. Eichler, J. Guttinger, M. I. Dykman, and A. Bachtold, Nat. Nanotechnol. **9**, 1007 (2014).
[21] E. Gavartin, P. Verlot, and T. J. Kippenberg, Nat. Commun. **4**, 2860 (2013).
[22] M. Sansa, E. Sage, E. C. Bullard, M. Gely, T. Alava, E. Colinet, A. K. Naik, L. G. Villanueva, L. Duraffourg, M. L. Roukes, G. Jourdan and S. Hentz, Nat. Nanotechnol. **11**, 552 (2016).
[23] A. N. Cleland and M. L. Roukes, J. Appl. Phys. **92**, 2758 (2002).
[24] K. Y. Fong, W. H. P. Pernice, and H. X. Tang, Phys. Rev. B **85**, 161410(R) (2012).
[25] Y. Zhang, J. Moser, J. Guttinger, A. Bachtold, and M. I. Dykman, Phys. Rev. Lett. **113**, 255502 (2014).
[26] F. Sun, X. Dong, J. Zou, M. I. Dykman, and H. B. Chan, Nat. Commun. **7**, 12694 (2016).
[27] B. H. Schneider, V. Singh, W. J. Venstra, H. B. Meerwaldt, and G. A. Steele, Nat. Commun. **5**, 5819 (2014).
[28] J. Atalaya, T. W. Kenny, M. L. Roukes, and M. I. Dykman, Phys. Rev. B **94**, 195440 (2016).
[29] A. W. Barnard, V. Sazonova, A. M. van der Zande, and P. L. McEuen, Proc. Natl. Acad. Sci. USA **109**, 19093 (2012).
[30] T. Miao, S. Yeom, P. Wang, B. Standley, and M. Bockrath, Nano Lett. **14**(6), 2982 (2014).
[31] F. Sun, J. Zou, Z. A. Maizelis, and H. B. Chan, Phys. Rev. B **91**, 174102 (2015).
[32] O. Maillet, F. Vavrek, A. Fefferman, O. Bourgeois, and E. Collin, New J. Phys. **18**, 073022 (2016).
[33] A. Vinante, Phys. Rev. B **90**, 024308 (2014).
[34] L. G. Villanueva, E. Kenig, R. B. Karabalin, M. H. Matheny, R. Lifshitz, and M. C. Cross, and M. L. Roukes, Phys. Rev. Lett. **110**, 177208 (2013).
[35] M. H. Matheny, M. Grau, L. G. Villanueva, R. B. Karabalin, M. C. Cross, and M. L. Roukes, Phys. Rev. Lett. **112**, 014101 (2014).
[36] H. J. R. Westra, M. Poot, H. S. J. van der Zant, and W. J. Venstra, Phys. Rev. Lett. **105**, 117205 (2010).
[37] K. J. Lulla, R. B. Cousins, A. Venkatesan, M. J. Patton, A. D. Armour, C. J. Mellor, and J. R. Owers-Bradley, New J. Phys. **14**, 113040 (2012).

[38] M. H. Matheny, L. G. Villanueva, R. B. Karabalin, J. E. Sader, and M. L. Roukes, Nano Lett. **13**(4), 1622 (2013).
[39] Y. Zhang and M. I. Dykman, Phys. Rev. B **92**, 165419 (2015).
[40] T. Rentrop, A. Trautmann, F. A. Olivares, F. Jendrzejewski, A. Komnik, and M. K. Oberthaler, Phys. Rev. X **6**, 041041 (2016).
[41] E. Collin, M. Defoort, K. Lulla, T. Moutonet, J.-S. Heron, O. Bourgeois, Yu. M. Bunkov, and H. Godfrin, Rev. Sci. Instrum. **83**(4), 045005 (2012).
[42] R. Lifshitz and M. C. Cross, *Reviews of Nonlinear Dynamics and Complexity*, edited by H. G. Schuster (Wiley-VCH, Weinheim, 2008), Vol. 1, pp. 1–52.
[43] See Supplemental Material at http://link.aps.org/supplemental/10.1103/PhysRevB.96.165434 for all the mathematical tools enabling quantitative fits and details on the experimental techniques.
[44] A. N. Cleland and M. L. Roukes, Sensors Actuators A **72**, 256 (1999).
[45] R. Almog, S. Zaitsev, O. Shtempluck, and E. Buks, Phys. Rev. Lett. **98**, 078103 (2007).
[46] A. N. Cleland, *Foundations of Nanomechanics* (Springer, Berlin, 2003).
[47] A. Berthelot, I. Favero, G. Cassabois, C. Voisin, C. Delalande, Ph. Roussignol, R. Ferreira, and J. M. Gérard, Nat. Phys. **2**, 759 (2006).
[48] M. I. Dykman, M. Khasin, J. Portman, and S. W. Shaw, Phys. Rev. Lett. **105**, 230601 (2010).
[49] T. K. Caughey, J. Acoust. Soc. Am. **35**, 1683 (1963).
[50] D. Cadeddu, F. R. Braakman, G. Tütüncüoglu, F. Matteini, D. Rüffer, A. Fontcuberta i Morral, and M. Poggio, Nano Lett. **16**, 926 (2016).